Charged particle production in $d+\mathrm{Au}$ collisions at $\sqrt{s_{NN}}=200$ GeV

Fu-Hu Liu*

Institute of Modern Physics, Shanxi Teachers University, Linfen, Shanxi 041004, China
and China Center of Advanced Science and Technology (World Laboratory), Beijing 100080, China

(Received 12 January 2004; published 7 June 2004)

We have given an explanation for the pseudorapidity distribution of charged particles produced in $d+\mathrm{Au}$ collisions at $\sqrt{s_{NN}}=200$ GeV [the maximum relativistic heavy ion collider (RHIC) energy]. A simple cylinder model is used in this paper which contains four components: leading projectile protons, leading target protons, cascade collisions in the gold spectator, and a cylinder. The model gives a good description for the experimental data obtained with the PHOBOS detector at RHIC. The high stage and high peak in the gold fragmentation region of the pseudorapidity distribution are contributed by the leading gold protons and the cascade collisions in the gold spectator, respectively.

DOI: 10.1103/PhysRevC.69.067901 PACS number(s): 25.75.−q, 24.10.Pa

The pseudorapidity distributions of charged particles produced in nucleus-nucleus collisions are important for understanding the evolution of the interacting system. In fixed target nucleus-nucleus collisions experiments [1–5], the pseudorapidity η is defined as $\eta=-\ln[\tan(\theta/2)]$, where θ is the emission angle of the concerned particle relative to the beam direction. In collider nucleus-nucleus collisions experiments [6–10], the same pseudorapidity definition is used, but θ is the emission angle relative to the direction of one beam. It is interesting for us to investigate the shape of the pseudorapidity distribution.

For a fixed target experiment at high energy, for example, for the nucleus-emulsion collisions at high energy, the pseudorapidity distribution of relativistic singly charged particles produced in central collisions can be fitted by a Gaussian distribution [11,12]. In noncentral nucleus-emulsion collisions at high energy, the pseudorapidity distribution of relativistic singly charged particles has to be fitted by two Gaussian distributions, one for produced particles and the other for leading protons produced in the projectile [13,14]. If the contribution of leading protons can be neglected, a Gaussian distribution gives a good fit for the pseudorapidity distribution.

For a collider experiment, for example for the Au+Au collisions at the relativistic heavy ion collider (RHIC), the pseudorapidity distribution of charged particles produced in central collisions can be fitted by two Gaussian distributions, one peak is in the $\eta>0$ region, and the other is in the $\eta<0$ region [8,9]. In noncentral Au+Au collisions at RHIC, the charged particle η distribution can also be fitted by two Gaussian distributions in the case of neglecting the contribution of leading protons.

However, recently, the minimum-bias pseudorapidity distribution of charged particles produced in collisions of deuterons (projectiles) with gold nuclei (targets) at a nucleon-nucleon center-of-mass energy $\sqrt{s_{NN}}$ of 200 GeV has to be fitted by a triple Gaussian distribution [15]. Even if we neglect the contributions of leading protons produced in deuterons and gold nuclei, a triple Gaussian fit is also needed. Some models, for example the microscopic model based on parton substructure [16], multiphase transport model [17,18], relativistic quantum molecular dynamics model [19], and parton saturation models [20] are inconsistent with the data [15], even if for the η distribution shape.

In order to give a description of the η distribution shape, we have developed a cylinder model in our previous work [21,22]. In this work, we shall use the cylinder model and consider the contribution of cascade collisions to give a description of the η distribution of charged particles produced in $d+\mathrm{Au}$ collisions at $\sqrt{s_{NN}}=200$ GeV [15].

Let us consider the process of high-energy nucleus-nucleus collisions. It is expected that one nucleus (projectile) and the other (target) make a cylindrical cut through each other along the direction of the incident projectile and form a participant [23]. The residual parts of the two nuclei remain relatively undisturbed forming spectators [23]. In rapidity space, in the center-of-mass reference frame or in the laboratory reference frame, the cylinder distributes to $[y_{\min},y_{\max}]$, where $y_{\min}$ and $y_{\max}$ are two endpoint rapidities of the cylinder. In the cylinder, the points with the same rapidity y_x form a emission plane (emission source). In the rest frame of the emission source, the particles are emitted isotropically. In the concerned reference frame, the η distribution of particles produced in the emission source with rapidity y_x will be

$$f(\eta,y_x)=\frac{1}{2\cosh^2(\eta-y_x)}, \tag{1}$$

where η is treated approximately as rapidity (y) due to that $\eta\approx y$ at high energy. The η distribution contributed by the cylinder can be given by

$$f_C(\eta)=\frac{1}{y_{\max}-y_{\min}}\int_{y_{\min}}^{y_{\max}} f(\eta,y_x)dy_x. \tag{2}$$

Let y_c denote the rapidity of participant-participant [23] center-of-mass and Δy denote the rapidity shift of two endpoints of the cylinder, we have $y_{\max}=y_c+\Delta y$ and $y_{\min}=y_c-\Delta y$. In $d+\mathrm{Au}$ collisions, the contribution of intranuclear

*Electronic address: liufh@dns.sxtu.edu.cn

cascade collisions in the Au spectator [23,24] has to be considered. As the first class approximation, the η distribution of cascade collisions is taken to be Eq. (2), but the rapidity shift is assumed to be δy. The contributions of leading protons produced in the projectile (d) and target (Au) have to be considered too. The leading proton η distribution is taken to be Eq. (1) with the rapidity shift Dy.

The contributions of leading projectile protons, leading target protons, cascade collisions in target spectator [23,24], and the cylinder are assumed to be k_P, k_T, k_{TT}, and $1-k_P-k_T-k_{TT}$, respectively. The normalized final η distribution can be given by

$$f(\eta) = k_P f(\eta, y_c + Dy) + k_T f(\eta, y_c - Dy) + \frac{k_{TT}}{\delta y}\int_{y_c-\delta y}^{y_c} f(\eta, y_x)dy_x + \frac{1 - k_P - k_T - k_{TT}}{2\Delta y}\int_{y_c-\Delta y}^{y_c+\Delta y} f(\eta, y_x)dy_x. \quad (3)$$

There are seven parameters y_c, Δy, δy, Dy, k_P, k_T, and k_{TT} in the normalized η distribution. If we consider a nonnormalized distribution, the eighth parameter will be need. Generally speaking, some of the parameters could be calculated according to the colliding geometry, stopping power [25,26], etc. For the purpose of convenience in this work, we regard all of them free parameters.

Equation (3) contains four components of the model. The cascade collision part and the cylinder part both have finite rapidity width from different endpoints, but the leading projectile and target parts have zero rapidity width from the endpoint. Considering the finite system and thus the randomness of the collisions, the participant protons will come from a different number of collisions, and each collision may have different strength (momentum transfer). Among the participant protons, the leading protons are protons with low momentum transfer, while the protons with intermediate or high momentum transfer will appear in the cylinder part as the nonleading protons. Protons produced in the spectator are also the leading protons with very low momentum transfer. We may say that the leading protons have near zero rapidity width from the endpoints because that all of them have the low momentum transfer. The zero rapidity width for the leading protons does not mean that the leading protons have the same rapidity. In fact, the distribution described by Eq. (1) is similar to a Gaussian distribution with a width of 0.91 [14].

The projectile and target parts in Eq. (3) have the same rapidity shift Dy (just opposite signs) due to the same low momentum transfer for the leading protons in the participant-participant center-of-mass reference frame. We are concerned about the momentum transfer, and for the leading protons the momentum transfer is low. Protons experience more collisions and have larger momentum transfer are not the leading protons, and the contribution of nonleading protons is considered in the cylinder part. Because both the leading protons from the deuteron and gold have low momentum transfer, we take the projectile and target parts in Eq. (3) to have the same rapidity shift. One may expect that participant protons from the deuteron tend to experience more collisions going through the larger gold nucleus, and then the rapidity distribution range of participant protons in the deuteron fragmentation region is wider than that in the gold fragmentation region.

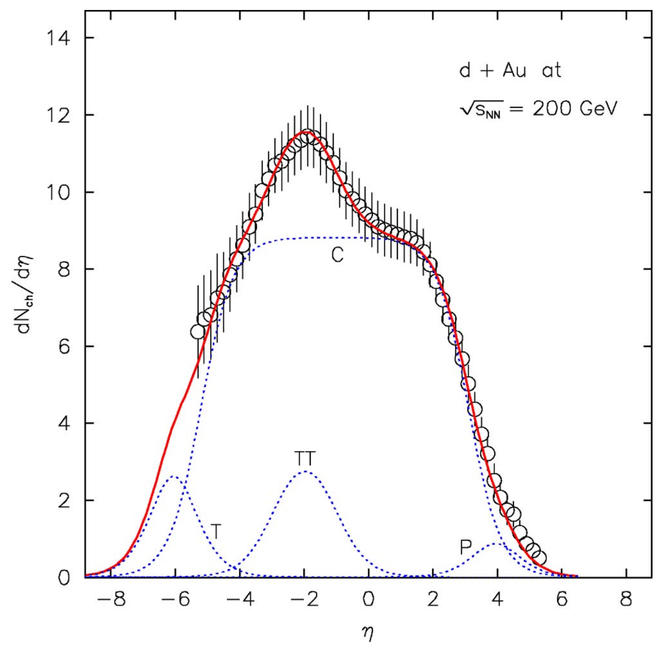

FIG. 1. (Color online) Pseudorapidity distribution of charged particles produced in d+Au collisions at $\sqrt{s_{NN}}=200$ Gev. The circles are the experimental data measured by Back *et al.* [15], and the curves are our calculated results.

Figure 1 presents the minimum-bias η distribution $dN_{ch}/d\eta$ of charged particles produced in d+Au collisions at $\sqrt{s_{NN}}=200$ GeV, where N_{ch} denote the multiplicity of charged particles. The circles are the experimental data measured by Back *et al.* and the emission angle is relative to the direction of the deuteron beam [15]. The data were obtained with the PHOBOS detector at RHIC and collected using the multiplicity array, covering $|\eta| \leq 5.4$ [15,27]. The solid curve is our result calculated by Eq. (3). In the calculation, we take $y_c=-1.05$, $\Delta y=4.15$, $\delta y=1.85$, $Dy=5.00$, $k_P=0.02$, $k_T=0.06$, $k_{TT}=0.08$, and the eighth parameter $N_{ch}=87.20$ with χ^2/degrees of freedom of 0.139. The contributions of leading projectile (d) protons, leading target (Au) protons, cascade collisions in the target spectator, and the cylinder are given in the figure by the dotted curves and marked by P, T, TT, and C, respectively.

From Fig. 1 one can see that Eq. (3) gives a good description for the minimum-bias η distribution of charged particles produced in d+Au collisions at $\sqrt{s_{NN}}=200$ GeV. The high stage in the gold fragmentation region is contributed to by the leading gold protons, and the high peak in the gold fragmentation region is contributed to by the intranuclear cascade collisions in the gold spectator. There are seven parameters for the normalized η distribution, and for the nonnormalized η distribution $dN_{ch}/d\eta$, eight parameters are needed. The experimental data presented in Fig. 1 can be fitted by a triple Gaussian distribution [15] with nine parameters, i.e., three peak positions, three widths, two fractions, and one normalization. Moreover, fitting the η distribution by a triple Gaussian distribution does not show a clear picture for the particle production.

For Au+Au collisions at the RHIC energies, two Gaussian distributions can fit the η distributions [6–10]. We have used a two-cylinder picture and described the η distribution in Au+Au collisions in our recent work [28–30]. The contributions of leading protons have been considered, and the contributions of cascade collisions have not been considered. In contrast to this work, we have divided the cylinder into two parts, namely, the target cylinder and the projectile cylinder, in our recent work [28–30]. In this study it is found that the cascade collisions in the gold spectator are important for d+Au collisions. It seems that they should be even more important for Au+Au collisions. However, in Au+Au collisions the cascade collisions can be neglected due to the relative small spectator in comparison with the participant. From the consideration of nuclear size and colliding geometry, the contribution of cascade collisions in the spectator in Au+Au collisions is estimated to be less than 1%. As for the cascade collisions in the spectator, there is no obvious inconsistency between the treatments of d+Au and Au+Au collisions from the cylinder model.

In order to exclude the effects of leading protons and cascade collisions, we suggest the experimental groups at RHIC to give the η distributions of negatively charged particles. Excluding the contribution of positive particles, the model prediction on the η distribution $dN_{\rm neg}/d\eta$ of negative hadrons produced in d+Au collisions at $\sqrt{s_{NN}}=200A$ GeV is shown in Fig. 2, where $N_{\rm neg}$ denotes the multiplicity of neagtive hadrons. In the calculation, we do not need to consider the contributions of leading protons and cascade collisions; and take the values of $y_{\rm c}$, Δy, and δy as the same as those for Fig. 1. The normalized constant $N_{\rm neg}$ is taken to be $(1-k_P-k_T-k_{TT})N_{\rm ch}/2\approx 36.62$, where k_P, k_T, k_{TT}, and $N_{\rm ch}$ are the parameters used for Fig. 1. From Fig. 2 we can see that the model prediction on the η distribution of negative hadrons in d+Au collisions at the RHIC energy has a wide plateau. This distribution is different from the solid curve in Fig. 1.

Accurately, the pseudorapidity and rapidity are not equal to each other for the nonzero mass particle. For particles emitted from a static isotropic source, the η distribution is $1/(2\cosh^2\eta)$. Equation (1) is, in fact, a result for massless particles. If we consider the relation between η and y for a particle with given mass [31], the relative fractions of pion, kaon, and proton, as well as the temperature are needed for analyzing the η distribution. For the purposes of convenience and reducing the parameter number, we have not distinguished η and y in the present work. The calculated error caused by $\eta\approx y$ is less than 7% if we regard all charged particles as pions and take a temperature of 300 MeV. Moreover, an express formula such as Eq. (3) cannot be obtained in the case of using an accurate relation between η and y [31]. We have to use the Monte Carlo method and statistics to obtain the η and y distributions in distingushing η and y [30].

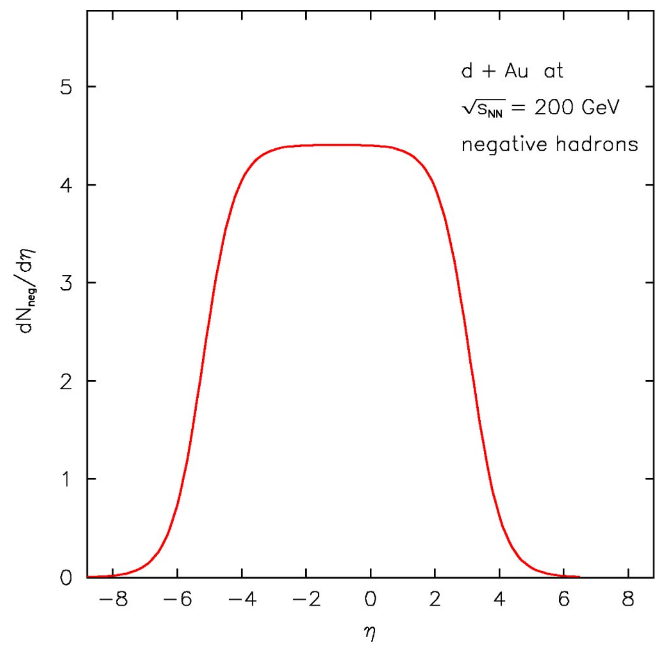

FIG. 2. (Color online) Model prediction on the pseudorapidity distribution of negative hadrons produced in d+Au collisions at $\sqrt{s_{NN}}$=200 GeV.

To conclude, we have given an explanation for the pseudorapidity distribution of charged particles produced in d+Au collisions at $\sqrt{s_{NN}}$=200 GeV. A simple cylinder model has been introduced in this work which contained four components: leading projectile protons, leading target protons, cascade collisions in gold spectator, and cylinder. Comparison with Au+Au collisions, the pseudorapidity distribution in d+Au collisions has a more complex structure. Both the contributions of leading gold protons and cascade collisions in gold spectator effect the pseudorapidity distribution. The high stage and the high peak in the gold fragmentation region are contributed by the leading gold protons and the cascade collision in the gold spectator, respectively. In order to exclude the effects of leading protons and cascade collisions, the negative particle pseudorapidity distributions in d+Au and Au+Au collisions at the RHIC energies are needed in the future.

This work was supported by the National Natural Science Foundation of China (NSFC) Grant No. 10275042, the Shanxi Scholarship Council of China Grant No. JLGB(2002)8-20021042, the Shanxi Provincial Foundation for Returned Overseas Scholars Grant No. JLGB(2001)15, the Shanxi Provincial Foundation for Natural Sciences Grant No. 20021006, and the Shanxi Provincial Foundation for Key Subjects Grant No. JJJC(2002)4.

[1] M. C. Abreu *et al.*, Phys. Lett. B **530**, 33 (2002).
[2] G. Singh, K. Sengupta, and P. L. Jain, Phys. Rev. Lett. **61**, 1073 (1988).
[3] M. I. Adamovich *et al.*, Phys. Rev. Lett. **62**, 2801 (1989).
[4] R. Albrecht *et al.*, Z. Phys. C **55**, 539 (1992).
[5] P. L. Jain, G. Singh, and K. Sengupta, Phys. Rev. C **43**, R2027 (1999).
[6] I. Arsene *et al.*, Phys. Rev. Lett. **91**, 072305 (2003).
[7] B. B. Back *et al.*, Phys. Rev. Lett. **89**, 222301 (2002).
[8] I. G. Bearden *et al.*, Phys. Rev. Lett. **88**, 202301 (2002).
[9] B. B. Back *et al.*, Phys. Rev. Lett. **87**, 102303 (2001).
[10] H. Ito for the BRAHMS Collaboration, Nucl. Phys. **A721**, 231 (2003).
[11] M. I. Adamovich *et al.*, Phys. Lett. B **201**, 397 (1988).
[12] M. I. Adamovich *et al.*, Phys. Lett. B **227**, 285 (1989).
[13] J. I. Nystrand *et al.*, Nucl. Phys. **A566**, 419c (1994).
[14] M. I. Adamovich *et al.*, Phys. Lett. B **352**, 472 (1995).
[15] B. B. Back *et al.*, nucl-ex/0311009.
[16] M. Gyulassy and X. N. Wang, Comput. Phys. Commun. **83**, 307 (1994).
[17] Z. W. Lin and C. M. Ko, Phys. Rev. C **68**, 054904 (2003).
[18] Z. W. Lin, S. Pal, C. M. Ko, B. A. Li, and B. Zhang, Nucl. Phys. **A698**, 375 (2002).
[19] H. Sorge, Phys. Rev. C **52**, 3291 (1995).
[20] D. Kharzeev, E. Levin, and M. Nardi, Nucl. Phys. **A730**, 448 (2004).
[21] F. H. Liu and Y. A. Panebratsev, Nucl. Phys. **A641**, 379 (1998).
[22] F. H. Liu and Y. A. Panebratsev, Phys. Rev. C **59**, 1798 (1999).
[23] R. J. Glauber, in *Lectures of Theoretical Physics*, edited by W. E. Brittin and L. G. Dunham (Interscience, New York, 1959), Vol. 1, p. 315.
[24] J. Hüfner, Phys. Rep. **125**, 129 (1985).
[25] G. E. Cooper for the NA49 Collaboration, Nucl. Phys. **A661**, 362c (1999).
[26] H. Weber, E. L. Bratkovskaya, and H. Stöcker, Phys. Rev. C **66**, 054903 (2002).
[27] B. B. Back *et al.*, Nucl. Instrum. Methods Phys. Res. A **499**, 603 (2003).
[28] F. H. Liu, Phys. Rev. C **66**, 047902 (2002).
[29] F. H. Liu, D. H. Zhang, and M. Y. Duan, Europhys. Lett. **61**, 736 (2003).
[30] F. H. Liu, Phys. Lett. B **583**, 68 (2004).
[31] C. Y. Wong, *Introduction to High-Energy Heavy-Ion Collisions* (World Scientific, Singapore, 1994), p. 25.